MCAT Institute
Progress Report
92-021

STUDY OF OPTICAL TECHNIQUES FOR THE AMES UNITARY WIND TUNNEL. PART 6. DIGITAL IMAGE PROCESSING

George Lee

January 1993

NCC2-716

MCAT Institute
3933 Blue Gum Drive
San Jose, CA 95127

TABLE OF CONTENTS 1

STUDY OF OPTICAL TECHNIQUES FOR THE AMES UNITARY WIND TUNNEL
PART 6. DIGITAL IMAGE PROCESSING

Summary

A survey of digital image processing techniques and processing systems for aerodynamic images has been conducted. These images covered many types of flows and were generated by many types of flow diagnostics. These include laser vapor screens, infrared cameras, laser holographic interferometry, Schlieren, and luminescent paints. Some general digital image processing systems, imaging networks, optical sensors, and image computing chips were briefly reviewed. Possible digital imaging network systems for the Ames Unitary Wind Tunnel were explored.

Introduction

Image processing of flow visualization images has been used for image enhancement and for quantitative flow analysis. Enhancement of wind tunnel flow pictures from Schlieren to infrared thermography is required in many instances because of the poor lighting and lack of optical access in most wind tunnels. This typically results in low contrast pictures which makes it difficult to distinguish flow details due to subtle contrast variations. The interpretation and analysis of the images are hampered. Digital image processing can be used for image enhancement. For example, standard techniques such as filtering, transforms, and thresholding are commonly used to improve the contrast. Noise and other unwanted features can be eliminated or reduced by image processing. Other image processing techniques such as edge detection and pattern recognition can be useful for the interpretation and analysis of the images. Digital image processing is also used for quantitative analysis in aerodynamics. The classical example is the analysis of interferograms from Mach-Zenher and laser holographic interferometry. Automated processing systems make fringe measurement a reasonable task. Digital image processing is used in infrared imagery to both enhance the image and to make measurements, e.g. boundary layer transition. Todays infrared camera systems come with image processing in many cases. Recently a new aerodynamic technique for global pressure measurement using pressure sensitive paints uses image processing as an integral part of the measurement. Model deformation measurements also

utilize image processing whether it is using stereo cameras or a tracker system.

The field of digital image processing is improving and expanding rapidly. It is being driven by consumer, commercial and industrial needs. These include among others, 3-D vision, electronic photography, desktop publishing, and medicine. With ever improving optical sensors, new generations of image processor chips, interactive data display and analysis software in conjunction with faster computers, an astonishing degree of image processing capability is available at relatively low cost. With the demonstrated need for digital image processing in aerodynamics and the availability of low cost commercial processor systems, the time is ripe to consider incorporating digital image processing in production wind tunnels like the NASA Ames Unitary Plan Wind Tunnel.

Purpose

The purpose of this study is to conduct a survey of digital image processing for aerodynamic flow visualization. Particular focus will be on those enhancement, restoration, and reconstruction methods that have been used in infrared imagery, interferometry, laser vapor screen, etc. General image processing schemes, especially those systems that can operate in real-time, will be surveyed. An image processor system for the Ames Unitary Plan Wind Tunnel will be explored.

Image Processing for Aerodynamics

1. Kudlinski and Park[1] describes NASA Langley's digital image processing laboratory and demonstrates the capabilities of the system with examples of images of vortices and flow through a nozzle. The system is based on a Gould IP 8500 image processor designed to process a large number of images fast enough for interactive work, figure 1. Notice the number of input and output devices. The Eikonix digitizing camera uses a 2048 linear photodiode array that scans in 2048 discrete steps to give a square pattern. A typical processing begins with (1) digitization of a photograph; (2) image enhancement with the IP 8500; and (3) output to display, storage or computer. The first example chosen for processing was a low contrast photograph, figure 2, of helicopter blade tip vortex in a smoke tunnel. In this photograph, the brightness variations or grey levels are proportional to the density variations. A histogram, figure

3, of this low contrast photograph is reflected in the small standard deviation of about 17. Most of the vortex had grey levels in a narrow range between 127 and 180 out of a total range of 256. Linear contrast stretching was used to improve the contrast by "clipping" grey levels values outside a specified range while "stretching" but preserving the ordering of the grey levels within the specified range. This was done interactively on the IP 8500. The user selects the two end points of the grey levels to be "stretched". Figures 4 and 5 show the enhanced image and its histogram. The standard deviation increased to 38 and the new image grey levels were stretched from 0 to 255. To further improve contrast, a standard image processing technique called histogram equalization was applied to the stretched image. Histogram equalization "consolidates" grey levels by assigning the same grey levels to pixels that differ by a small amount to produce a more uniform grey level distribution. This latter enhancement did not improve the image because the grey level was too low. To see the density variations within the vortex, an interactive grey level "slicing" was applied. Essentially this maps the constant grey level contours, and thus highlights the key structural features of the vortex. It was found that a low-pass filter helped in reducing noise in the image. The final enhanced image is shown in figure 6. Of course, pseudo color could be another alternative to grey level slicing.

Figures 7 and 8 show the same sequence of image processing applied to a vortex photograph taken by the water vapor screen method. Note the vast improvements achieved. The final case was the enhancement of a computer generated image of flow through a nozzle. The computer color coded the Mach number contours. After image processing, the Mach number contours were much sharper, see figures 9 and 10.

2. John Schriener[2] of the Ames Aerodynamics Division has been studying vortices from fighters at high angle of attacks with the laser vapor screen method. Typical photographs of the vortices are shown in figures 11 and 12. The images were digitized on a small personal computer and pseudo color was used to highlight the vortex structure. Figure 12 shows several vortex cross-sections along the model. In many cases, "linking" of the cross-sections to create a three-dimensional vortex to see the vortex interaction with the model is highly desirable. The "linking" processing algorithm is a higher form of image processing that needs further development. Edge detection is another powerful enhancement technique to define

structure and surface boundaries. Roberts, Sobel and Laplac operators are some of the common edge detectors that are used. More accurate operators such as "Canny"[3] was designed for our "Fringe Analysis System". A discussion of edge detection is given in references 4 to 7. Most digital image processing text books[8,9] will give the fundamentals of edge enhancement. Vortices were edge detected on the Fringe Analysis System using the Canny algorithm, figure 13. The Canny scheme is slow, taking several minutes. An array processor or the next generation computers will speed up the process.

3. Interferometry: Digital image processing is an absolute necessity for any realistic data reduction scheme for interferometry. Interferograms of aerodynamic flow fields from the classical Mach Zehnder or more recent laser holographic method[10] generates very complicated fringe patterns. In many cases, noise and low contrast compounds the situation. A typical interferogram of an airfoil is shown in figure 14. To obtain quantitative data, the fringes must be digitized, fringe centers measured, ordered, and numbered[11]. Usually, this requires filtering of noise, enhancement of fringes, and segmentation of fringes. Even with today's image processors with special algorithms, the task remains difficult.

Over the last decade, NASA Ames has developed two image processors for fringe analysis. This first system[12] used a De Anza image processor connected to a VAX 11/780 computer, figure 15. It has 512 x 512 pixel resolution with 8 bit intensity and 2 image storage planes with graphic and alphanumeric overlay. It can perform addition, subtraction and comparisons of images. Output includes monitors, printer, plotter, and terminal. The second generation system[13] uses an Imaging Technology board on a Micro-VAX II minicomputer. It was developed as a turnkey system by KMS Fusion, Inc. of Ann Arbor, Michigan. The resolution is 512 x 512 pixels with 8 bit intensity with 8 image storage planes. Capabilities include pixel location, histogram equalization and stretching, max. and min. grey levels, standard deviation, zoom, patch, and edge detection. It can measure fringes along any given line and for the entire image. There are output monitors, tape, ethernet, and provisions for printer.

Torres[14] used the first image processor to digitize a series of airfoils as an optical technique to measure airfoil pressures. A

polygon is drawn along the upper and lower surfaces of the airfoil. The scale factor and an initial point is chosen and the digitization of the fringes takes a few seconds. For images of good contrast with sharp and well defined fringes, the derived pressures agreed well with transducer measured pressures. For poorer images and for regions where the fringe intensity is too high, i.e. merge together, the results were poor and further image enhancements were needed.

Examples of images processed with the KMS Fusion system are given next. Figure 16 is an interferogram of an airfoil at transonic speeds. Note the high intensity of fringes at the nose of the airfoil. To digitize fringes in the nose region, image magnification by "zooming" in with the image processor is used. This figure illustrates the automatic identification of the center of the fringes (a vertical and a horizontal line was chosen for the image processor to locate the fringes). Notice that the processor cannot distinguish between the dark fringes and any black object. Hence the operator must interactively make corrections. Figure 17a shows a fringe pattern that has been converted to a binary image by thresholding. Filtering is used to clean up noisy areas, figure 17b. Finally, the center of the fringes were determined. Figure 18 shows the fringe center lines superimposed on the original image. Several algorithms for fringe center locations have been tried, e.g. gradient methods, steepest decent, thresholding, slope reversal and linking. Fringes within a boundary layer are shown in figure 19.

The fringe processing techniques can also be used for oil flow patterns. In most oil flow patterns, the lines of oils are very fine and closely spaced together. This may pose a problem but may be resolved by suitable magnification of the image. A variation of the oil flow technique: the "oil dot" method where small dots of oil are placed on the model to form widely spaced oil streaks to define the surface flow could be used. This type of pattern can be easily resolved by a fringe analysis processor.

4. Bouchary[15], et al. of ONERA applied digital image processing of infrared images for boundary layer transition detection. Shown in figure 20 are IR images of a wing. The left image has a transition pattern that is barely visible while the image on the right is strongly visible as the turbulent wedges can be seen. For strong images, no enhancement is required and the transition location is easily determined. For weak images, enhancement by averaging of a

sequence of images can be done in real-time to improve the signal to noise ratio. Typically a factor of four improvement can be achieved by averaging the pixel intensity. For images where averaging is not sufficient, time-delayed methods such as histogram equalization was used. When equalization was performed on a very narrow part of the histogram, details of specific parts of the image were seen. Color coding was another way to see the laminar, transition, and turbulent regions. Another technique which seems to work for very small changes in intensities was to plot the pixel intensity along the chord of the wing, figure 21. Small changes in grey levels, about 4 out of a total of 256 can be detected. Knowing the flow goes from laminar to transition to turbulent, the transition point can be found.

Two other methods, sublimation and liquid crystals are used for transition detection. These two techniques give very similar images as the infrared method. Obviously, similar digital image processing techniques can be used.

5. Digital image processor is also an integral part of the pressure-sensitive paint technique currently being developed for aerodynamic pressure measurements[16,17]. A schematic of two approaches is given in figure 22a. One uses ultra violet light while the other uses laser light to excite the paint. The paint then emits light (luminesces) which is imaged by a camera. A 512 x 512 resolution, extremely low-light detection with an image processor was used to analyze and display the paint response in real-time, giving a visualization of surface pressures. A typical image is shown in figure 22b.

Due to low-light levels and poor signal-to-noise ratios of video cameras, image enhancement is required. Morris averaged 100 video frames and in that image five adjoining rows of pixels were averaged to determine the luminescence. To account for noise due to CCD dark current, image subtraction of the "dark" image was performed. To determine the pressures, the "flow-on" image is mapped on the "flow-off" image by the image processor. One major problem in the mapping is that the "flow-on" image can be distorted as the model is deformed by the aerodynamic loads. This registration of the image requires image processing algorithms which have not been resolved yet.

6. Cho and McLachlan[18] used digital image processing to determine instantaneous 2-D velocity fields via the laser light sheet/particle streak method. The original photograph and the enhanced image are shown in figure 23 of flow behind a cylinder. An image processing system using an IBM PC, a real-time Imaging Technology frame grabber, and image processing software "Image Lab" and "Image Tech" by Werner Frei Associates was developed for this problem. The streak pattern was processed by contrast manipulation, noise cleaning, filtering, statistical differencing, thresholding, etc. This photograph was also processed by the KMS Fusion image processor using the Canny edge detector algorithm, see figure 24. Note the similarities between the two images. The good streaks were processed interactively on the screen for velocity determination. Noise from the camera and noise introduced during the image enhancement process were corrected by a coordinate transformation.

7. Cho[19] later developed a new technique, "digital image velocimetry" to measure instantaneous velocity fields. A time sequence of images are taken with a high-speed camera. Images were digitized, enhanced and superimposed to construct an image equivalent to a particle-streak image. A simple example of a double-exposure image is shown in figure 25. With the large numbers of particles, it is extremely difficult to follow individual particles to measure the displacements necessary for velocity determination. The new technique digitally Fourier transform the particle image into fringes, figure 26 for velocity determination.

8. Imaging processing was applied by Wallace, et al.[20] to study the turbulent structure of a boundary layer on a flat plate. In this experiment, smoke was injected through a rearward facing slot and a 5 watt argon-ion laser was used to create a light sheet. The light was swept by a rotating mirror to match the frequency of a 16mm movie camera. The image was enhanced in two ways. First, the maximum grey level (white) was assigned to regions with highest gradient and the minimum value (black) was assigned to regions of lowest gradients with 255 grey levels in between, figure 27b. This was use of thresholding and equalization. This technique highlights the outer and inner smoke frontiers. The second enhancement technique adds the digitized positive and negative of the same image after offsetting two pixels between the images. The result is an image that shows a base relief effect which accentuates the interior structure, figure 27a.

9. Gennero and Mathe[21] constructed a real-time edge detection system at ONERA. The system consisted of a CCD camera, digitizer and an Apple II computer. Images of vortices in the wake of a model were taken by the laser vapor screen method, figure 28. A simple threshold scheme by which the operator can interactively adjust the digitized image to its binary form, i.e. threshold set to either 1 or 0. The edge detector is the Haar 3x3 operator. The process takes 20 milliseconds and can handle 2 images.

Brandt[22] used a simple edge detection based on discrimination of high values of spatial derivatives between adjacent derivatives. Temporal derivatives of the turbulent jet was obtained by subtraction of two sequential video frames to show the high turbulence of the jet , see figure 29.

KMS Fusion used the Canny edge detector for Schlieren pictures to detect shock waves, figure 30.

10. Image processing is also an integral part of model deformation measurement systems. For example, Meyn used hitograms to set the contrast of the images interactively. The Langley stereo-camera system used a thresholding scheme to remove background noise so that target coordinates can be accurately calculated by their centroid.

I of NEWT

The Integration of Numerical and Experimental Wind Tunnel is a concept being proposed by John Schreiner and the Advance Aerodynamic Concept Branch. It is a facility designed to exploit the capabilities of both wind tunnel and computational fluid mechanics. Using various types of flow diagnostics and a high-speed network to tie the experimental data to the computer facilities, I of NEWT facility will provide real-time understanding of the aerodynamics of the model being tested. It will give the wind tunnel customer better data and allow the wind tunnel to be operated more efficiently. A sketch of the proposed system is shown in figure 31.

The top of the sketch shows some of the imaging subsystems. A high-speed network ties the experimental data to theoretical, storage, and display portions of the facility. The imaging subsystems

function as sensors, digital image processors, image analyzers, and formatting for output. It can also contain image storage and image display devices. Since this paper is on digital image processing, we shall address only the imaging subsystems and some of the high-speed networks for transmitting image data.

Imaging Systems

A basic digital image processing system consists of a sensor to detect the object, an image processor to enhance and process the image, analyze the data, and provide data storage and output for display. Image processing system can be classified by the type of sensors being used. For wind tunnel applications, there could be high-speed cameras operating at hundreds to thousands of frames per second, real-time video cameras operating at 30 frames per second, and still cameras operating at single shot to several frames per second. For most wind tunnel applications, real-time and stills will be used.

1. Real-time video: Todays real-time image processing system typically consists of a CCD video camera, a frame grabber on a PC, and storage and display. Strum[23] believes that today about 75% of the image processing are done with such systems. Mulgronkar and Gable[24] describes a conventional imaging network, figure 32, which consists of cameras, image processors, display and storage devices, network and a host bus to connect the devices and other peripherals. A common resolution is 512x512 pixels with 8 bit pixel intensity. The resolution is barely adequate for most wind tunnel applications. Higher resolutions at 1024x1024 are being made commercially. But consider that at 512x512x8 pixel resolution, 7,864,320 bytes per second of processing is required. Color imaging at 512x512x16 bit resolution is also available. Strum gives a list of image processing subsystems with their features and costs in table I.

The type of computing platform for image processing for aerodynamics is open. There are several engineering workstations that could be used. These include the IBM PC, DEC Micro VAX. II, Sun Microsystem and HP workstations. Some of the requirements, according to Wager[25], for a standard platform would include:

- simple, but powerful interfaces
- high resolution, high-speed graphics

- ease of use
- state-of-art hardware and software
- third-party hardware and software available
- low cost, high performance

2. Still cameras: The Kodak DCS digital camera system offers a 1024x1280 pixel full-frame CCD images. It can take color and black and white digital images with quality and resolution approaching that of film. It is mounted on a Nikon F-3 camera. It takes up to 6 images in one burst at 2.5 images per second and can store 158 uncompressed images or 600 compressed images. Figure 33 illustrates the imaging chain of the system. Images from the digital DCS or DCS 200 cameras go to a microcomputer with Aldus Photo Styler software for PC and Adobe Photoshop software for Macintosh. It can also be interfaced to a workstation. Storage is provided by an image library. Output includes prints, color images, transparencies, etc. The system can access images from photographic film via the RFS 2035 scanner.

- Kodak also makes the VIDEK Megaplus camera designed for high resolution scientific applications. It is a CCD array of 1320x1035x8 pixels with 6.8 micron square pixels with 100% of the sensor area being light-sensitive. It uses an electronic strobe which can be triggered to capture an image at any desired moment. It can operate at a maximum frame rate of 6.9 per seconds. The VIDEK camera is compatible with many commercial frame grabber based and image processing systems such as the VIDEK Mega Plus interactive Image Pro software suitable for many scientific and engineering applications. The latest Megaplus, model 4.2 has improved resolution to 2029x2044x8 pixels.

- Microcomputer Power sells a solid state "pSEE high resolution camera with 2048x2048x8 pixels that captures an entire image at the same time instead of the normal pixel by pixel or line by line format. The system includes the camera, imaging board for a PC, and processing software. Output can be viewed on high-resolution monitors and stored on disk.

- Photometrics, Ltd., makes a 2048x2048 pixel CCD camera and 12 bits per pixel. (It uses an Eastman Kodak sensor.) Software for camera control, image acquisition, and calibration, and interface with PC and Macintosh is provided.

Advanced Image Processing

1. Forckheimer[26] describes a 2nd generation of "smart optical sensor" that combines sensing and processing on the same semiconductor chip. The chip includes circuitry for A/D conversion and digital image processing such as filtering, edge detection, histograming, correlation, etc. at up to 100 frames per second. Simpler tasks such as binary template matching could be performed much faster. This chip has over 500,000 transistors and can be mounted like a conventional CCD sensor. It was designed to be used in an IBM PC environment with a library for traditional image processing operations. Routines can be linked to the user's C-program to facilitate the development of user applications. It was designed to be operated in an industrial situation.

2. Processor chips: Gove[27] discussed the need for inexpensive programmable image processing chips that can do image computing functions at up to video rates. Industry analysts project that by 1993, nearly one-half of the image processors will be single-chip image computing. Figure 34 illustrates some of the functions and uses of image computing chips. Some of the current processor chips are given in Table II. Gove proposes a new "highly-integrated architecture for single-chip image computing for future applications. When coupled with advanced memories, image acquisition and image display devices, it is projected that processing speeds of 2 billion operations per second can be possible. Image computing functions that now require supercomputers can be done with single chips.

3. Network: In the future, higher resolutions and real-time operation will require the need for high-speed networks for image processing. Mulgronkar and Gable[24] describe an image processing workstation that includes a high-speed bus, high-speed array processors, and a high-performance and high-storage disk of many Gigabytes. A high-speed network, VisiNET, developed by Recognition Concepts Inc. is designed for high-resolution, real-time operation. This system is shown in figure 35.

- Schneider and Strack[28] describe their "apART" system, figure 36, which is an open, distributed network. It has the X window, a SUN workstation, optical disc, etc. and support of different image interchange formats.

4. Image compression: Image compression is a method used to efficiently code the image data to reduce the number of bits required to represent an image. Thus, there will be less storage memory needed and reduce the image transmission requirement. The need for image compression for aerodynamics is obvious. High resolution is required but in many applications, e.g. Schlieren, IR, etc., there is a significant amount of redundancy in the data. The image compression can be used effectively. Razavi, et al.[29] describes a still picture compression chip set which performs image compression and expansion. Rabbani and Jones[30] gives a general survey of compression techniques.

Recommendations

1. IR image processing will probably be used for boundary layer transition detection and for temperature measurements in support of the pressure sensitive paints. The recently purchased IR camera has routine image enhancement software. The IR camera probably lacks resolution for some of the anticipated applications. This is one area that will require further attention.

2. The RA Division has PC based image processors for general flow visualization such as vapor screen and Schlieren. The image processing software that is commercially available should be sufficient for general applications. These video image processing systems will be the most useful system for wind tunnel applications. Work should be geared toward the development for vapor screen and Schlieren.

3. The RA Division has a dedicated image processor, "FAS", for fringe analysis from interferograms and oil flow pictures. This system has been little used because interferometry and oil flow are seldom used. However, the "FAS" system should be maintained for future use.

4. Higher resolution still cameras with image processors will definitely be needed for model deformation measurements. The area of research should be pursued.

5. When I of NEWT facility activities accelerate, image processing, high-speed networks, etc. will become more important. Preliminary studies of this area should be undertaken.

References

1. Kudlinski, R. A., and Park, S. K.: "Digital Enhancement of Flow Field Images," NASA TP 2770, 1988.

2. Weber, B. J., Schreiner, J. A., and Gilbaugh, B. L.: "A 10-watt Laser Diode Light Sheet Projector for Flow Visualization," FED, vol. 108, ASME 1991.

3. Canny, J.: "A Computational Approach to Edge Detection," IEEE Transaction on Pattern Analysis and Machine Intelligence, vol. PAMI-8, no. 6, Nov. 1986.

4. Torre, V., and Poggio, T.: "On Edge Detection," IEEE Transactions on Pattern Analysis and Machine Intelligence, vol. PAMI-8, no. 2, 1986.

5. Nalwa, V. S., and Binford, T. O.: "On Detecting Edges," IEEE Trans. Patt. and Mach. Intell., vol. PAMI-8, no. 6, 1986.

6. Lunscher, W. H. H. J., and Beddoes, M. P.: "Optimal Edge Detector Design I: Parameter Selection and Noise Effects," and "Optimal Edge Detector Design II: Coefficient Quantization," IEEE Trans. Patt. Anal. Mach. Intell., vol. PAMI-8, no. 2, 1986.

7. Davis, L.: "A Survey of Edge-Detection Techniques," Computer Graphics Image Processing, vol. 4, 1975.

8. Schalkoff, R. J.: "Digital Image Processing and Computer Vision," John Wiley, N.Y. 1989.

9. Horn, B. K. P.: "Robot Vision," MIT Press, McGraw-Hill, 1986.

10. Lee, G.: "Real-Time Laser Holographic Interferometry for Aerodynamics," NASA TM 89462, 1987.

11. Lee, G.: "A Tomographic Technique for Aerodynamics at Transonic Speeds," NASA TM 86766, 1985.

12. Becker, F., and Yu, Y. H.: "Digital Fringe Reduction Technique Applied to the Measurement of Three Dimensional Transonic Flow Fields," Opt. Eng., vol. 24, no. 3, 1985.

13. Downward, J. G., et al.: "Modular Digital Fringe Analysis System," KMS Fusion no. 02202 under NASA contract NAS2-12531.

14. Torres, F. J.: "Application of Digital Holographic Interferometry to Pressure Measurements of Symmetric, Supercritical, and Circulation Control Airfoils in Transonic Flow Fields", NASA TM 88358, 1987.

15. Bouchary, A. M., et al.: "Processing of Infrared Thermal Images for Aerodynamic Research," 1983 Int. Tech. Conf. Geneva, Switzerland, April 18-22, 1983.

16. Morris, M. J., et al.: "Aerodynamic Applications of Pressure-Sensitive Paint," AIAA 92-0264, 1992.

17. McLachlan, B. G., et al.: "Pressure Sensitive Paint Use in the Supersonic High-Sweep Oblique Wing (SHOW) Test," AIAA 92-2686, 1992.

18. Cho, Y-C, and McLachlan, B. G.: "Personal Computer (PC) Based Image Processing Applied to Fluid Mechanics Research," Proc. SPIE, vol. 829, 1987.

19. Cho, Y-C.: "Digital Image Velocimetry," SPIE 32nd International Tech. Symp. Opt. Optoelec. Appl. Sci. Eng., San Diego, CA, Aug. 1988.

20. Wallace, J. M., et al.: "Applications of Image Processing Analysis to the Study of the Turbulent Boundary Layer Structure," Flow Visualization III, Hemisphere Pub. 1983.

21. Gennero, Ch., and Mathe, J. M.: "Real Time Edge Extraction Application to the Study of Vortices Cores," Flow Visualization III, Hemisphere Pub., 1983.

22. Brandt, A.: "Hydrodynamic Flowfield Imaging," Flow Visualization III, Hemisphere Pub., 1983.

23. Strum, W. E.: "Trends in Microcomputer Image Processing," SPIE, vol. 900, 1988.

24. Mulgronkar, R., and Gable, S.: "Real-time Digital Disk and High Speed Network in Image Processing," SPIE, vol. 900.

25. Wagner, G.: "The Macintosh as an Image Processing and Analysis Workstation," SPIE, vol. 1258, 1990.

26. Forchheimer, R., et al.: "MAPP 2200 - A Second Generation Smart Optical Sensor," SPIE, vol. 1659, 1992.

27. Gove, R. J.: "Architectures for Single-Chip Image Computing," SPIE, vol. 1659, 1992.

28. Schneider, V., and Strack, R.: "apART: System for the Acquisition, Processing, Archiving, and Retrieval of Digital Images in an Open, Distributed Imaging Environment," SPIE, vol. 1659, 1992.

29. Razavi, A., et al.: "A Low Cost Still Picture Compression Chip Set," SPIE, vol. 1659, 1992.

30. Rabbani, M., and Jones, P. W.: "Digital Image Compression Techniques," SPIE, vol. TT7.

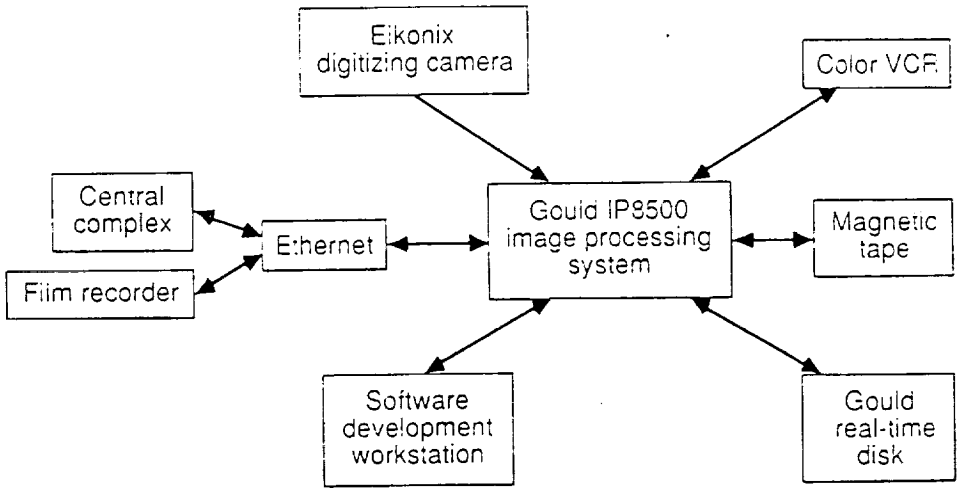

Figure 1. NASA Langley Image Processor (after Kudlinski)

Figure 2. Photograph of Vortex (after Kudlinski)

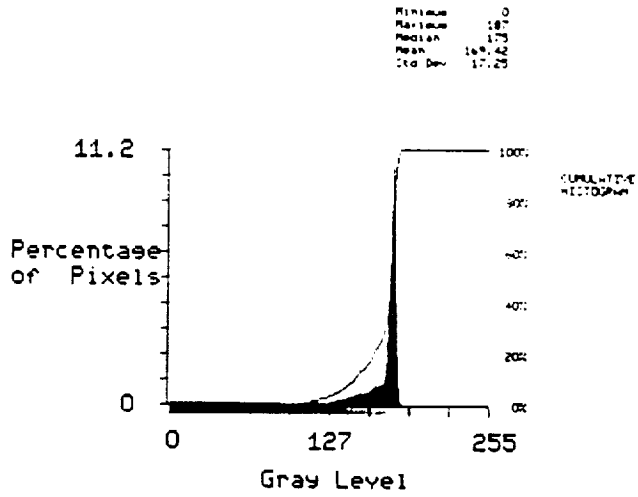

Figure 3. Histogram of Vortex Image (after Kudlinski)

Figure 4. Contrast Stretched Image (after Kudlinski)

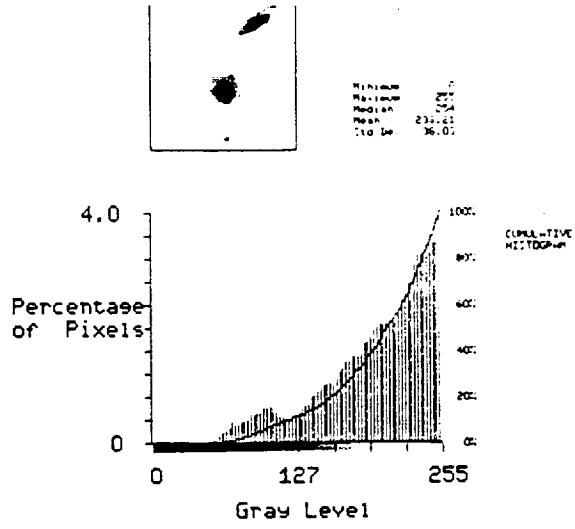

Figure 5. Histogram of Stretched Image (after Kudlinski)

Figure 6. Enhanced-Contoured Image (after Kudlinski)

Figure 7. Photograph of Water Vapor Screen Vortex (after Kudlinski)

Figure 8. Enhanced Vortex (after Kudlinski)

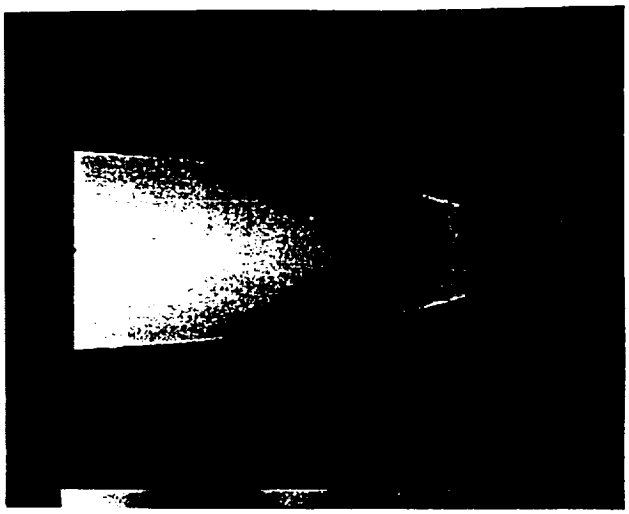

Figure 9. Computer Generated Nozzle Flow (after Kudlinski)

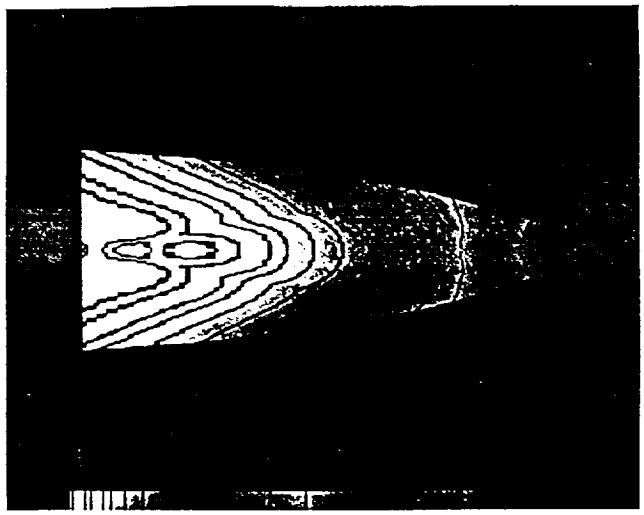

Figure 10. Enhanced Nozzle Mach Contours (after Kudlinski)

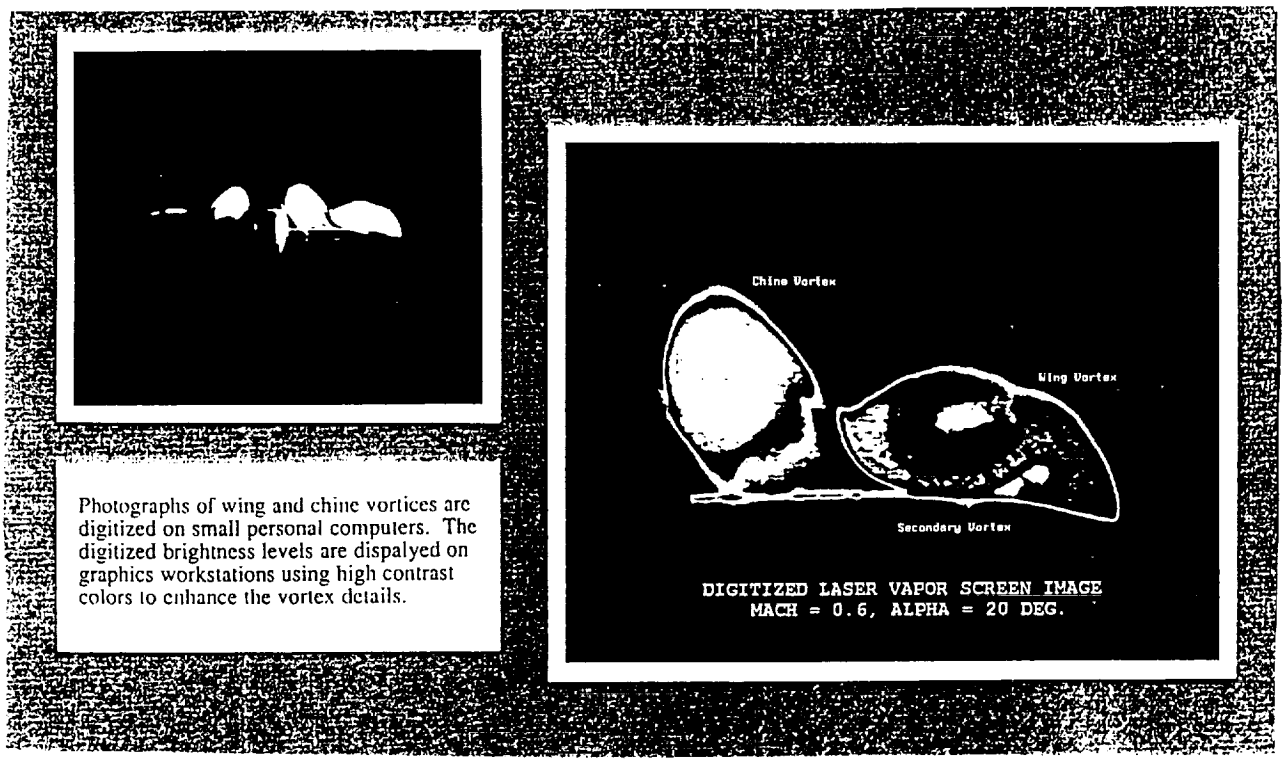

Figure 11. Photograph and Digitized Vortex Images (after Kudlinski)

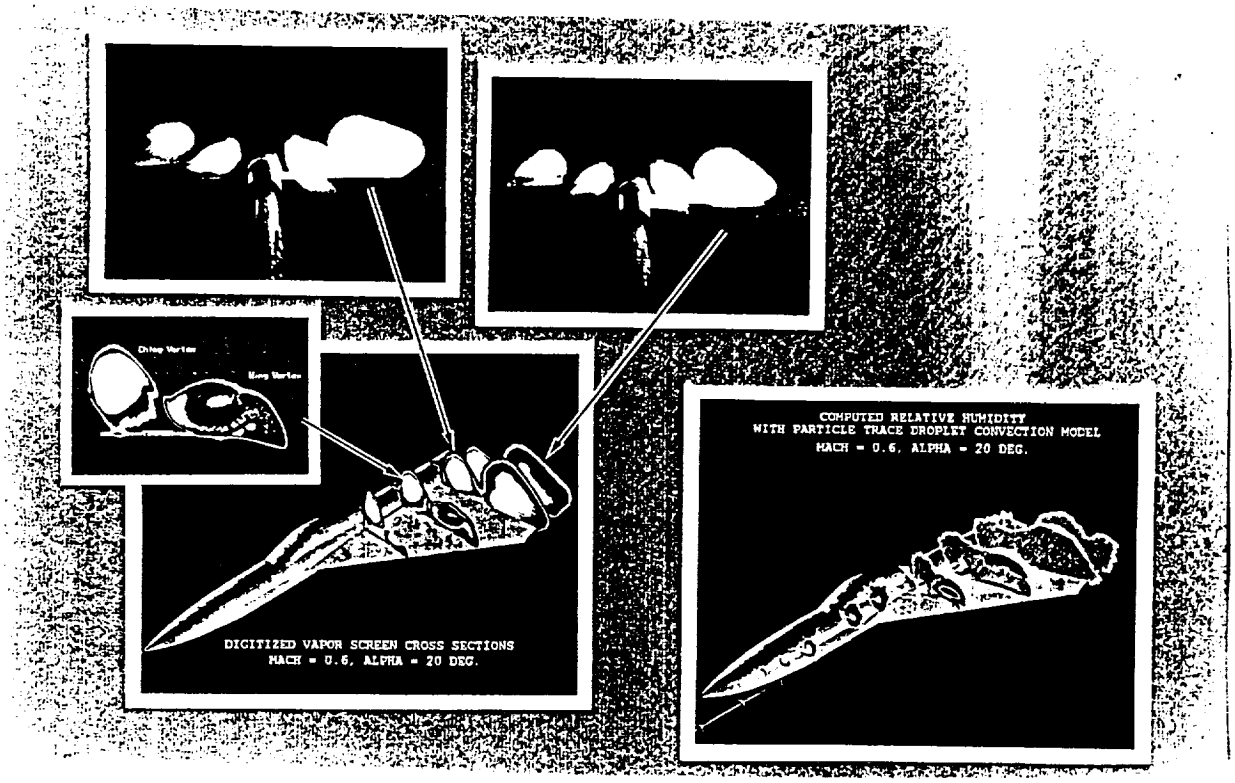

Figure 12. Photographs and Mapped Vortex Images (after Schriener)

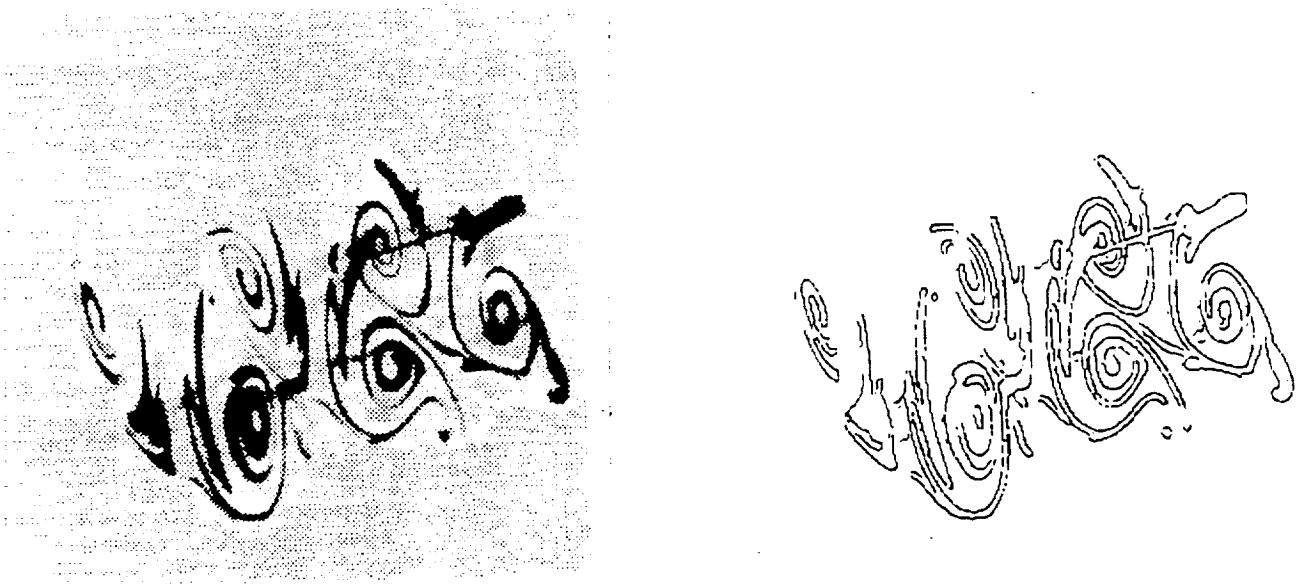

Figure 13. Edge Detection by Canny (after Downward)

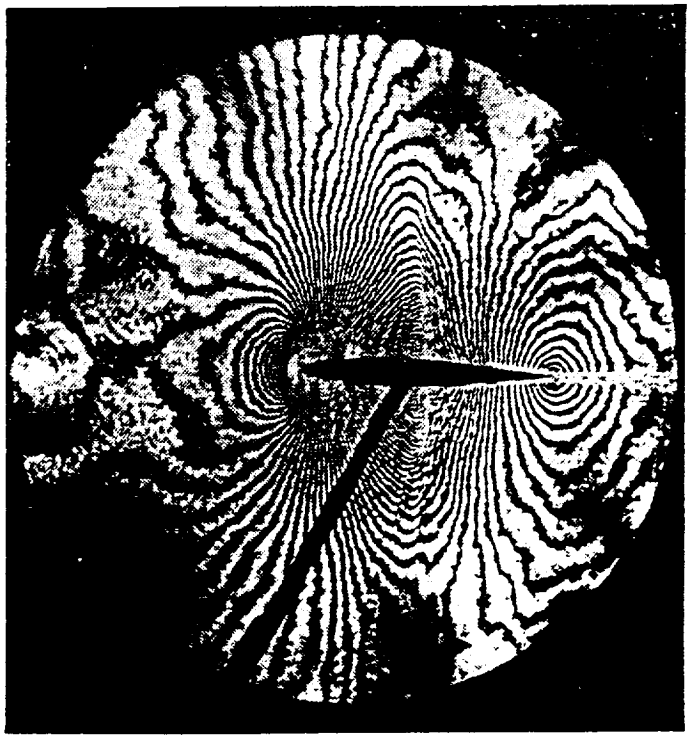

Figure 14. Interferogram of an Airfoil (after Lee)

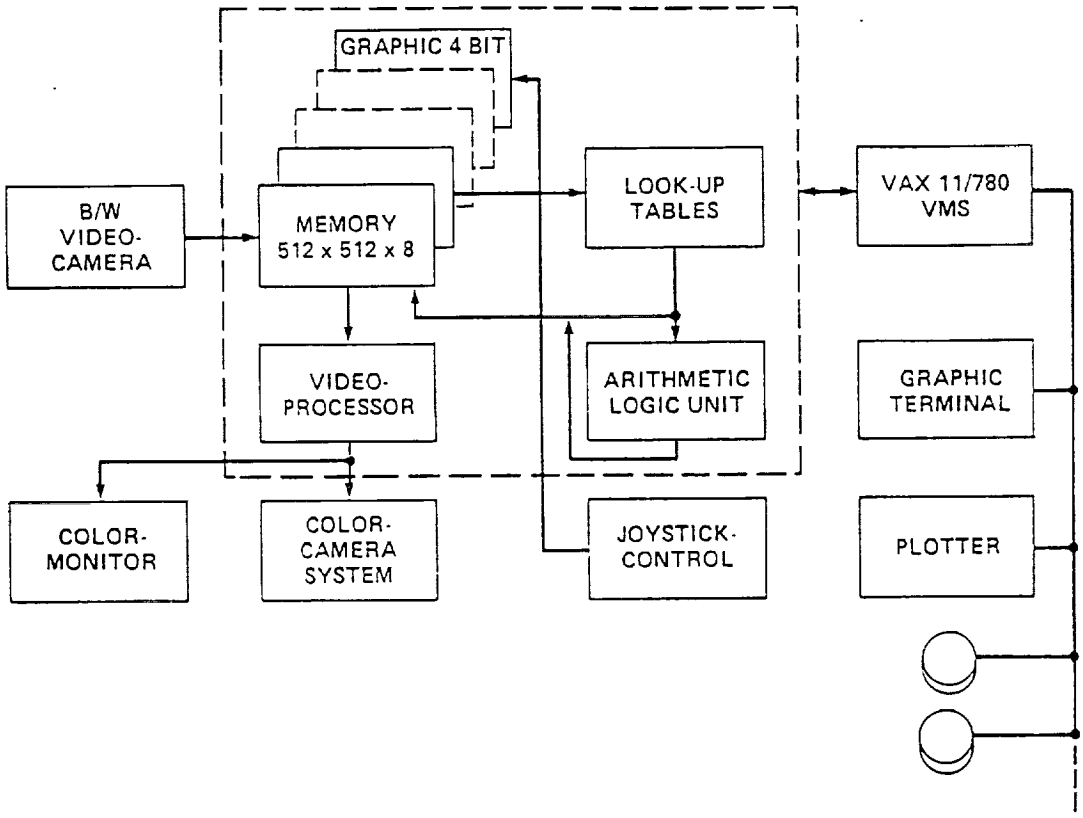

Figure 15. De Anza Image Processor (after Torres)

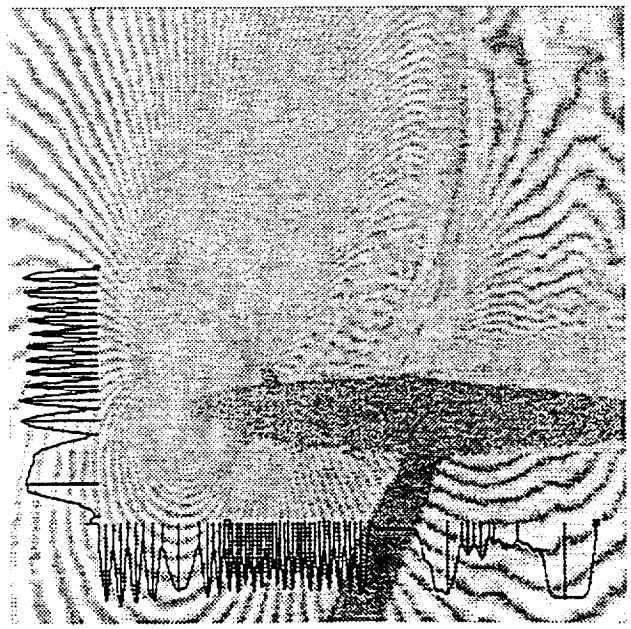

Figure 16. FAS Processed Airfoil (after Downward)

Figure 17a. Binary Processed Fringes (after Downward)

Figure 17b. Filtered Fringes

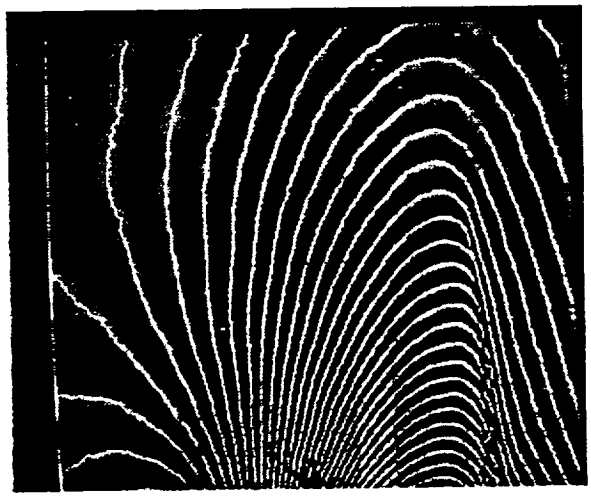

Figure 18. Fringe Centers Located (after Downward)

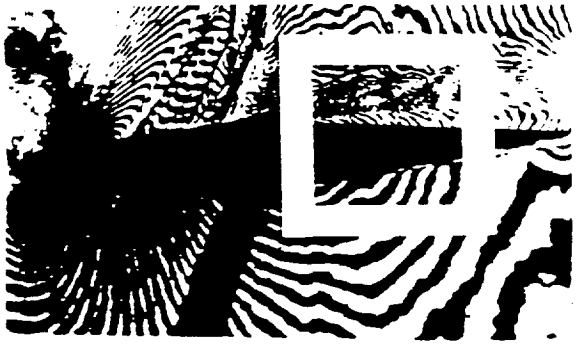

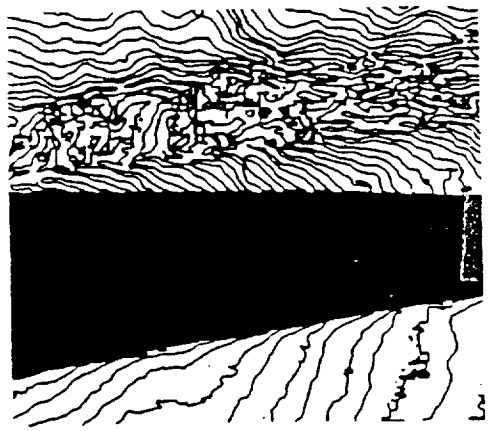

Figure 19. Boundary Layer Processed (after Downward)

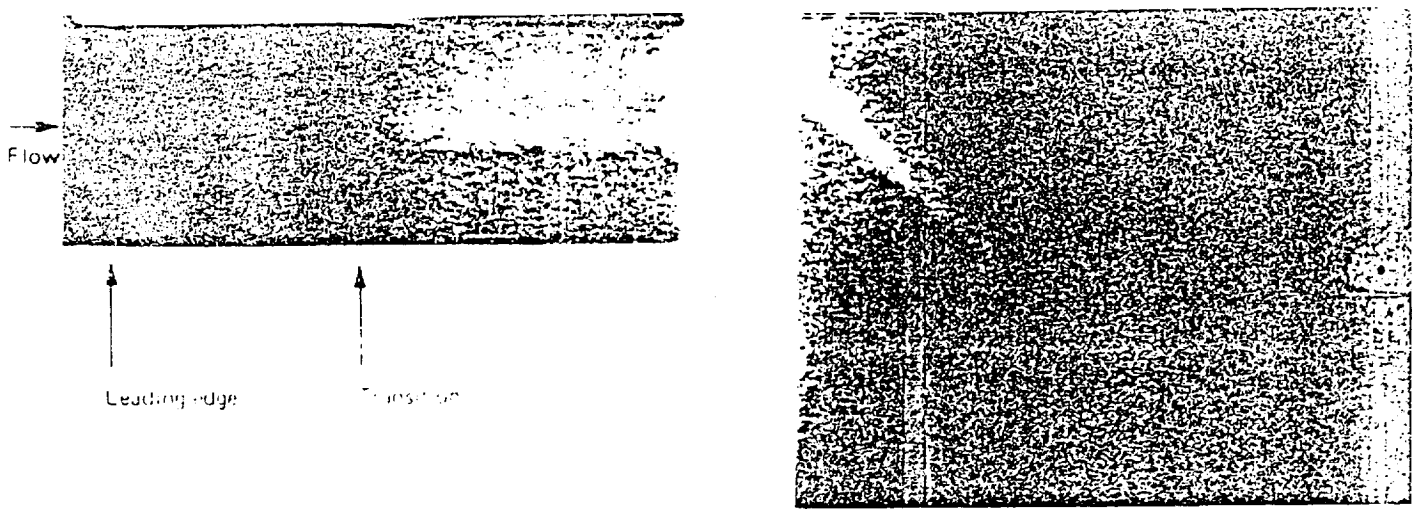

Figure 20. IR Images of Wing (after Bouchary)

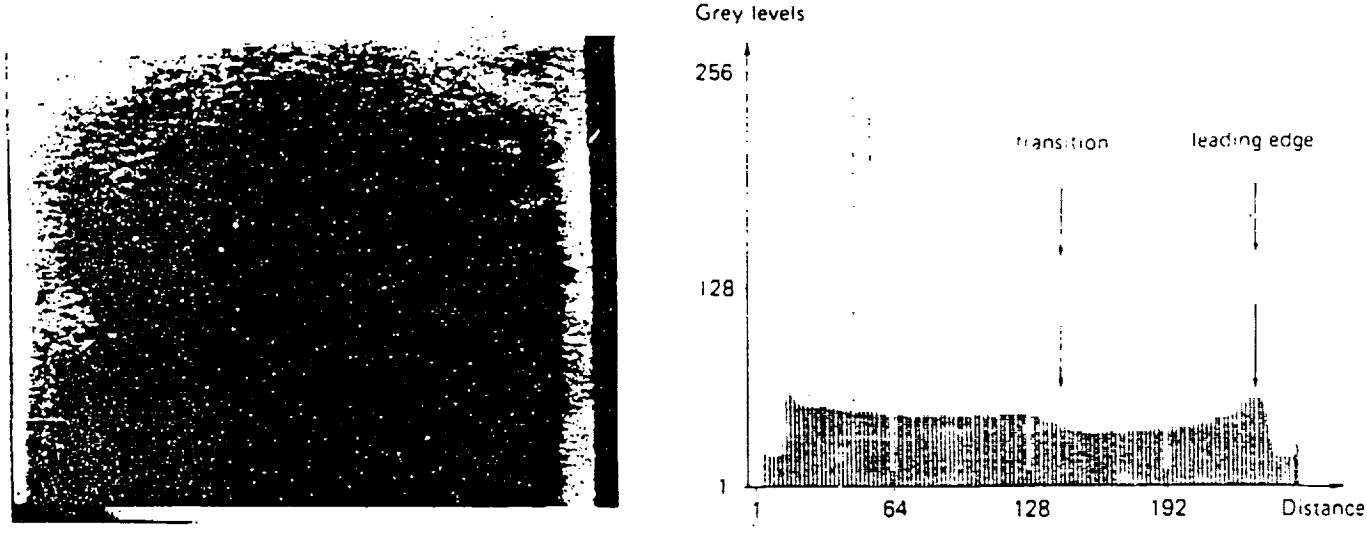

Figure 21. Pixel Intensity Distribution (after Bouchary)

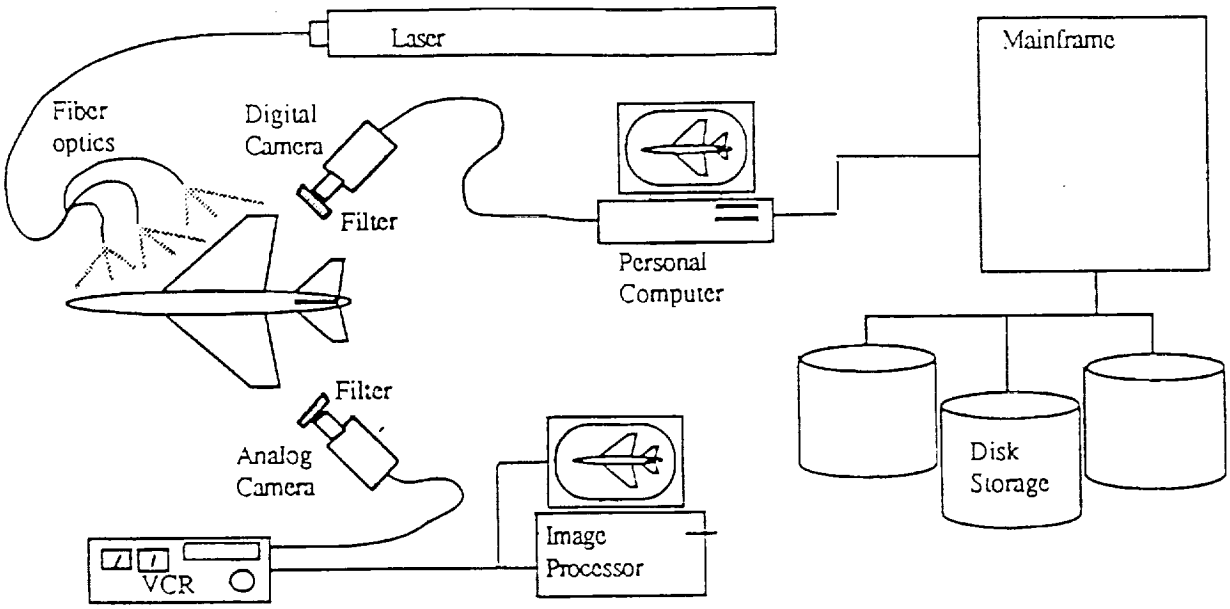

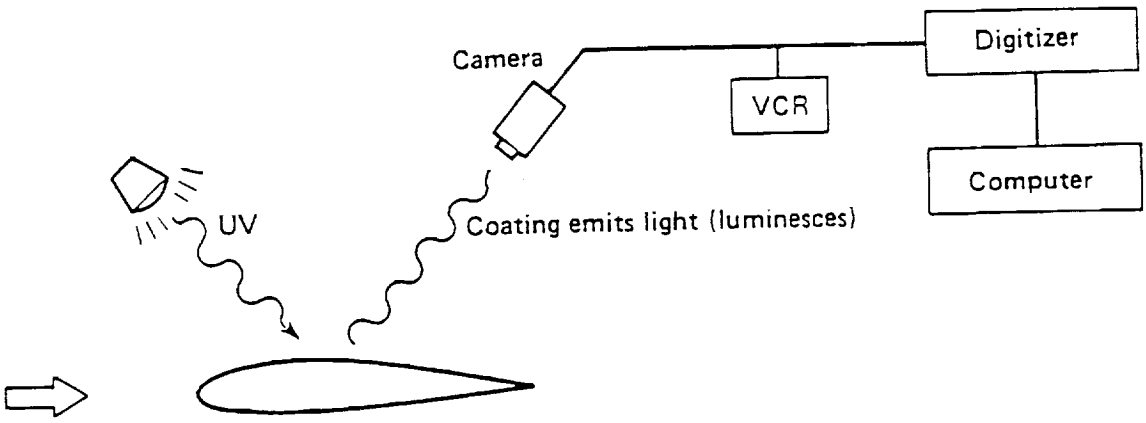

- Luminescence intensity depends on oxygen partial pressure
- Mole fraction of oxygen in air is known
- Video/photo + image processing to measure intensity, thus mapping surface pressure

Figure 22a. Pressure Sensitive Paint Image Processing (after Morris, McLachlan)

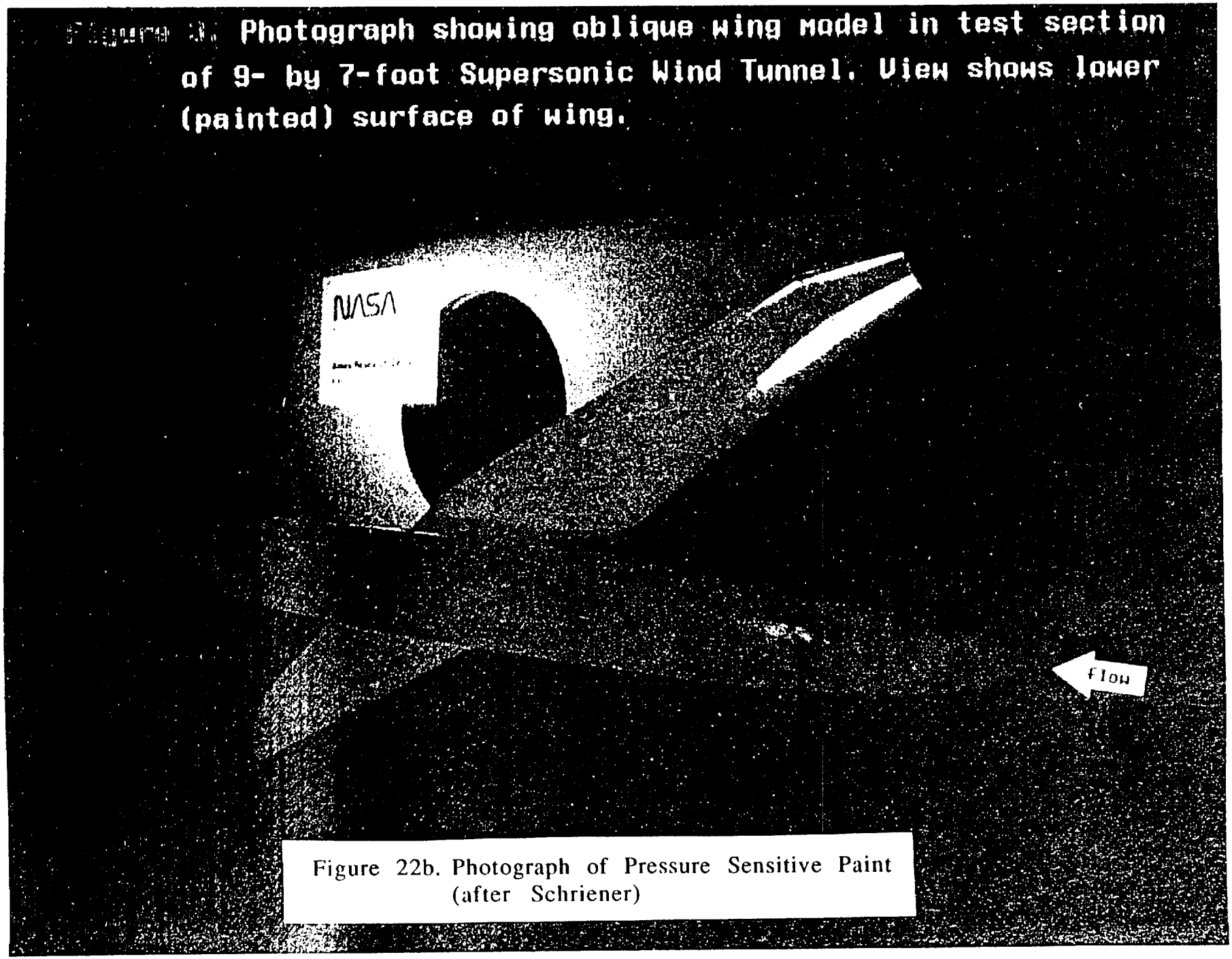

Figure 22b. Photograph of Pressure Sensitive Paint (after Schriener)

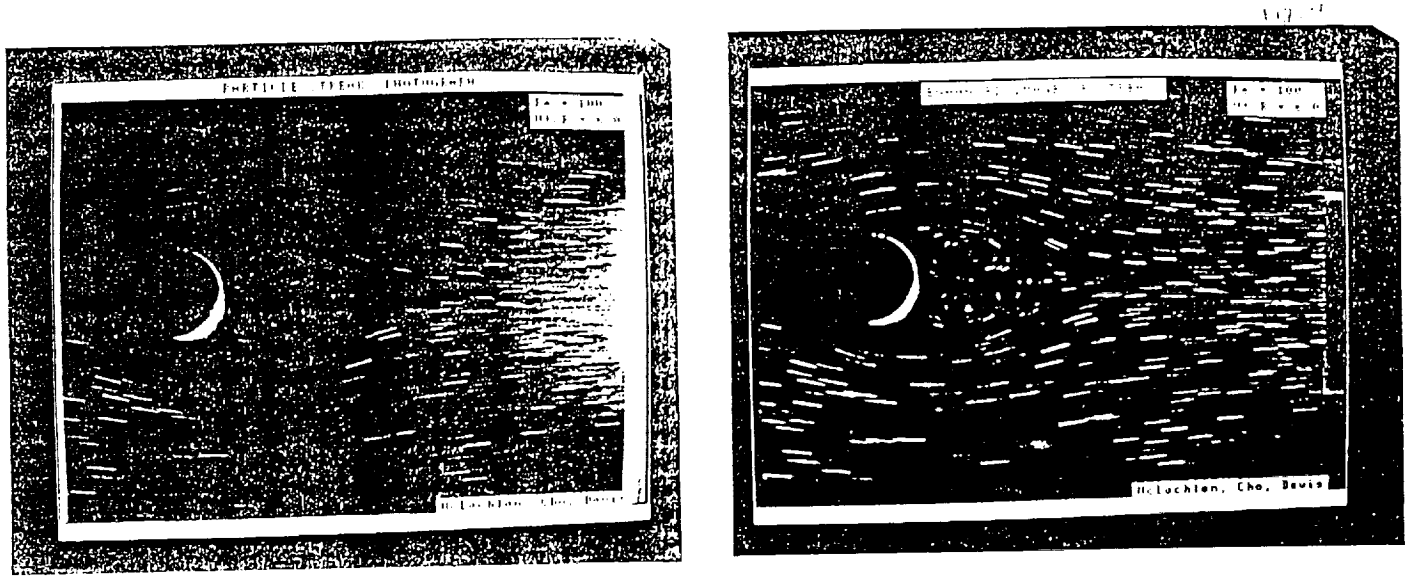

Photograph

Enhanced Image

Figure 23. Photograph and Enhanced Image of Particle Streak Flow Behind Cylinder (after Cho)

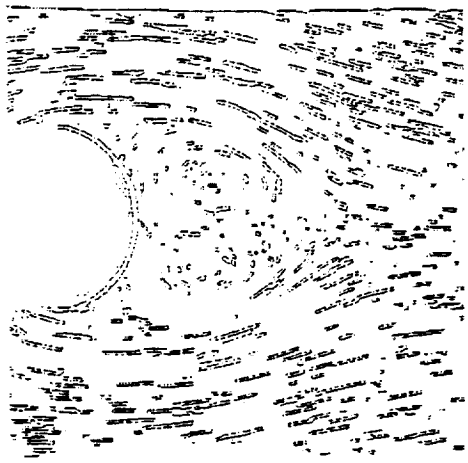

Figure 24. Canny Edge Detected Image of Cylinder Flow (after Downward)

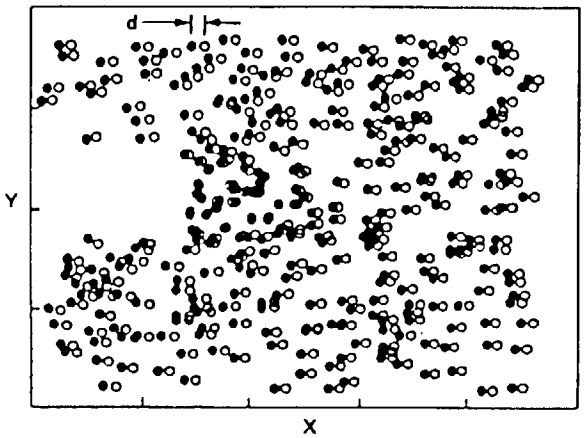

Figure 25. Double-Exposed Image of Cylinder Flow (after Cho)

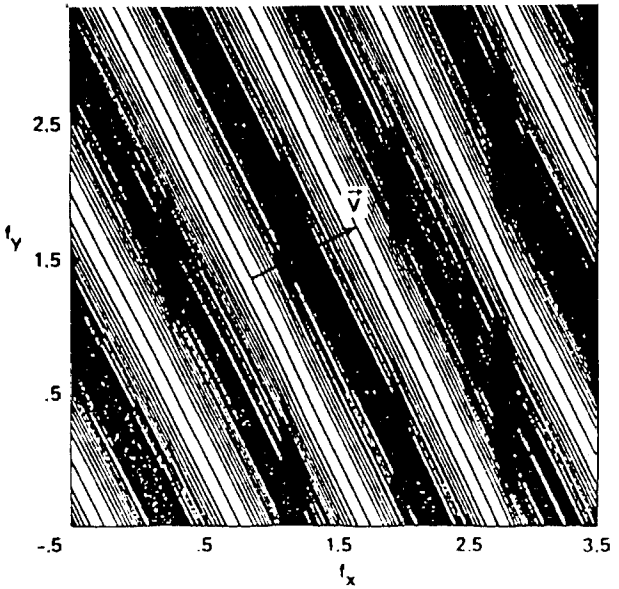

Figure 26. Cylinder Flow Image Processed into Fringes (after Cho)

Figure 27a. Photograph of Turbulence in Smoke Flow (after Wallace)

Figure 27b. Base-relief Image of Turbulence

Figure 28. Edge Detection of Vortex (after Gennero)

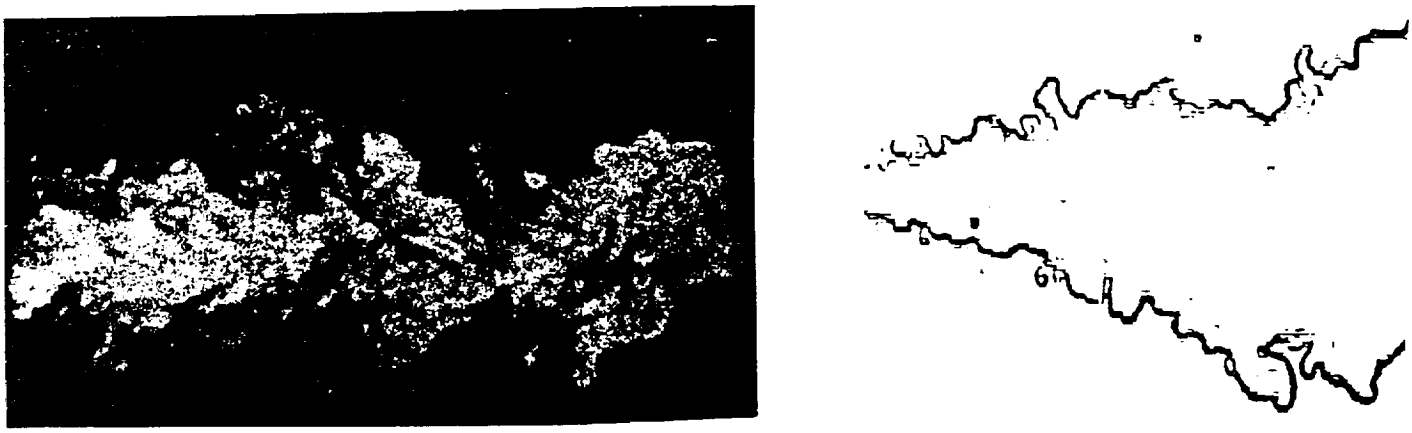

Figure 29. Edge Detection of Jet (after Brandt)

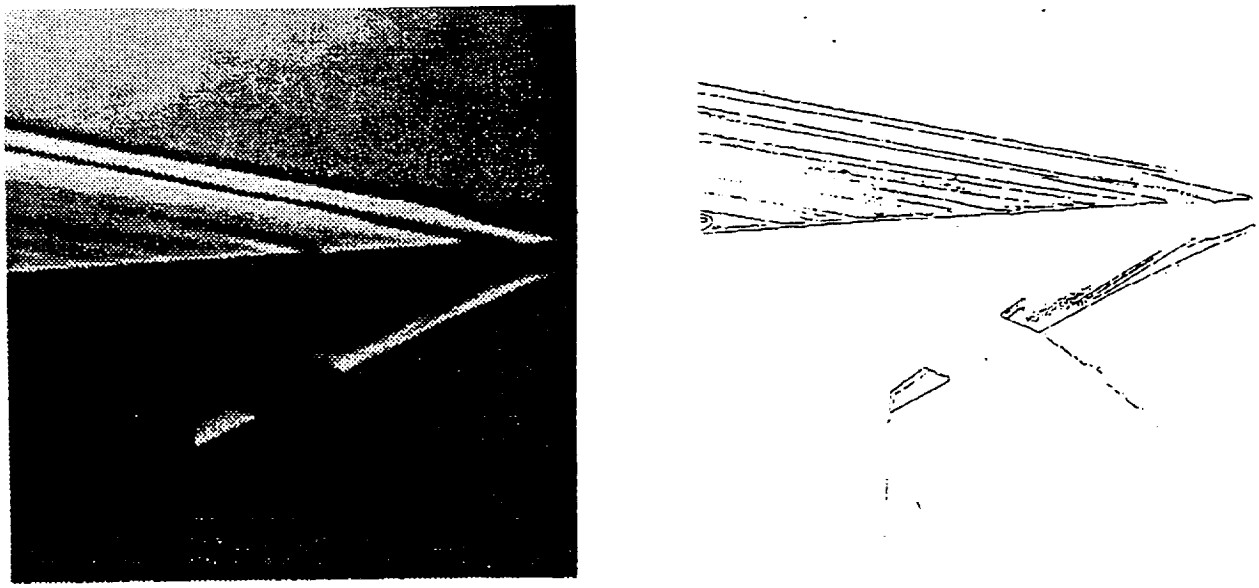

Figure 30. Edge Detection of Shocks (after Downward)

INTEGRATION OF NUMERICAL AND EXPERIMENTAL WIND TUNNELS
(I of NEWT)

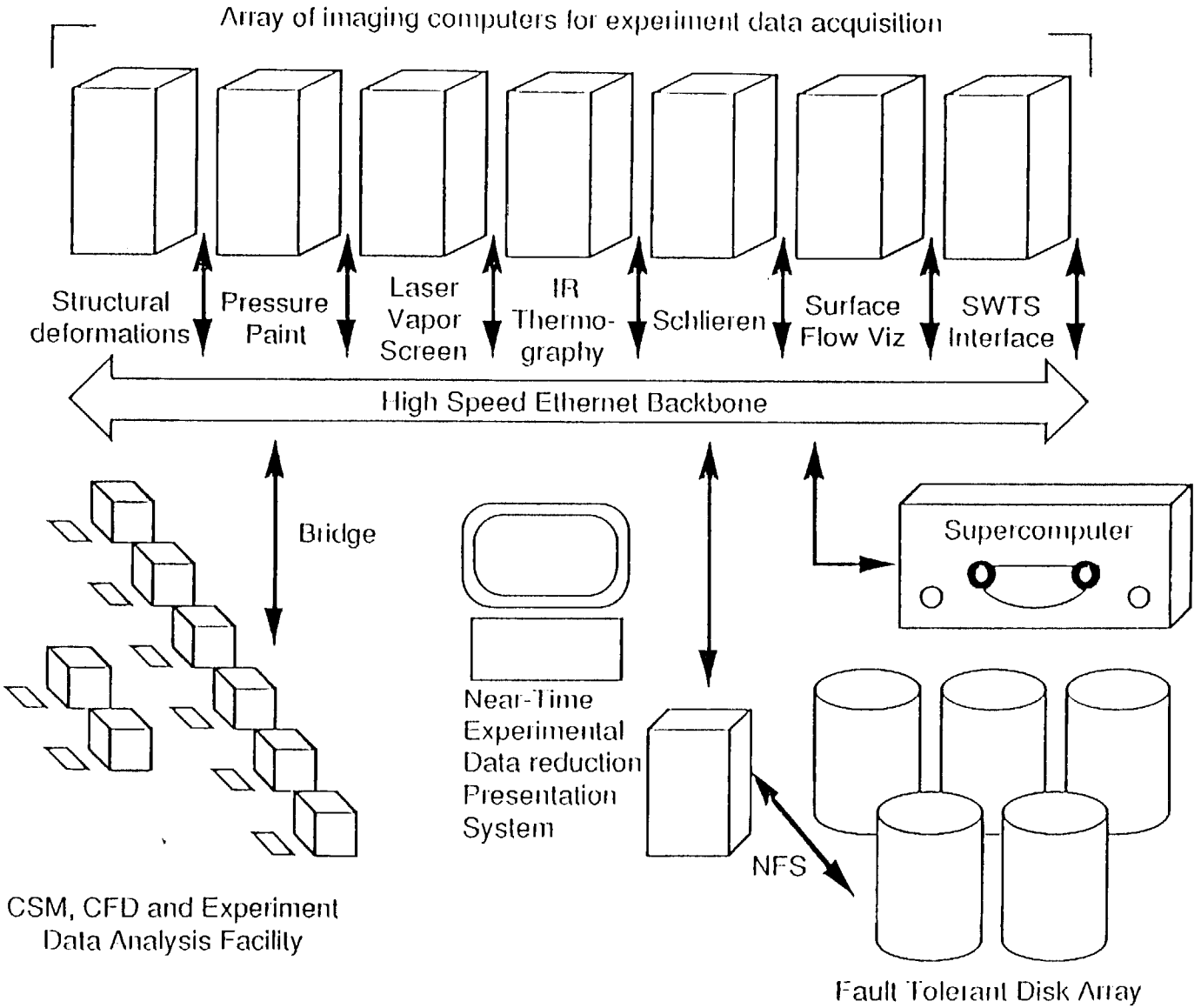

Figure 31. I of NEWT (after Schriener)

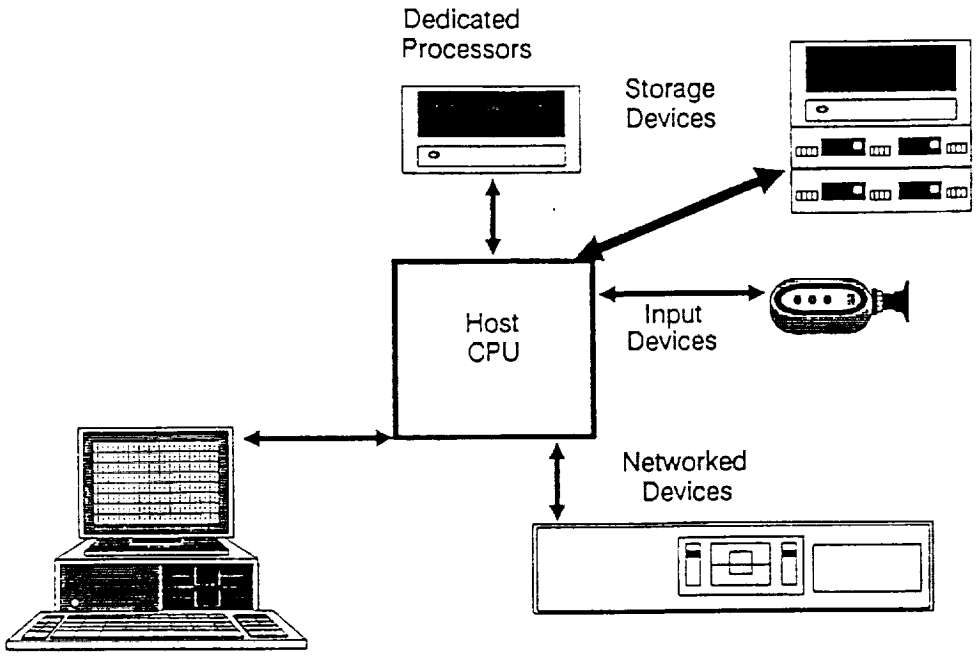

Figure 32. Convention Imaging Network (after Mulgronkar)

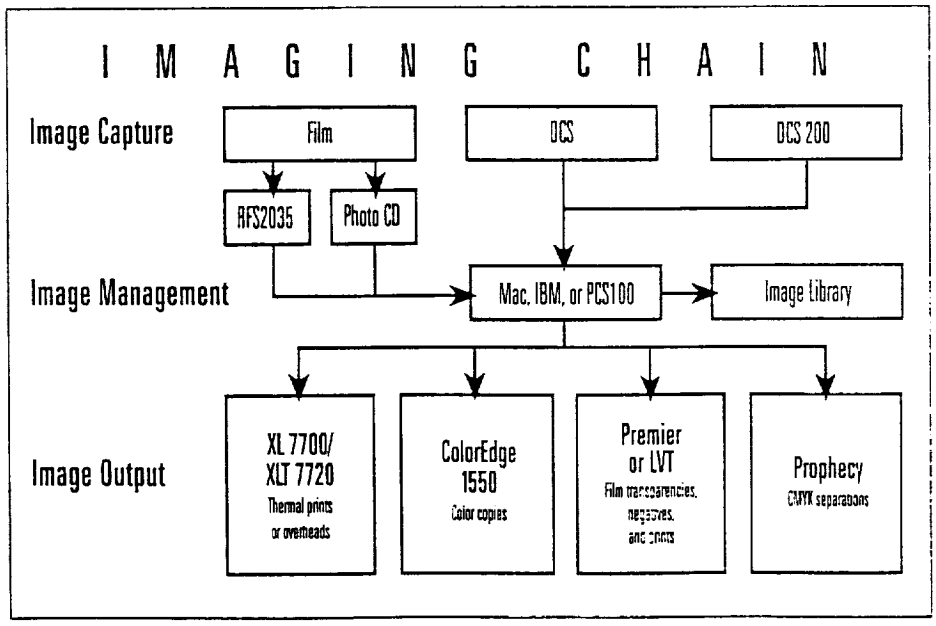

Figure 33. Kodak Digital Camera (after Kodak)

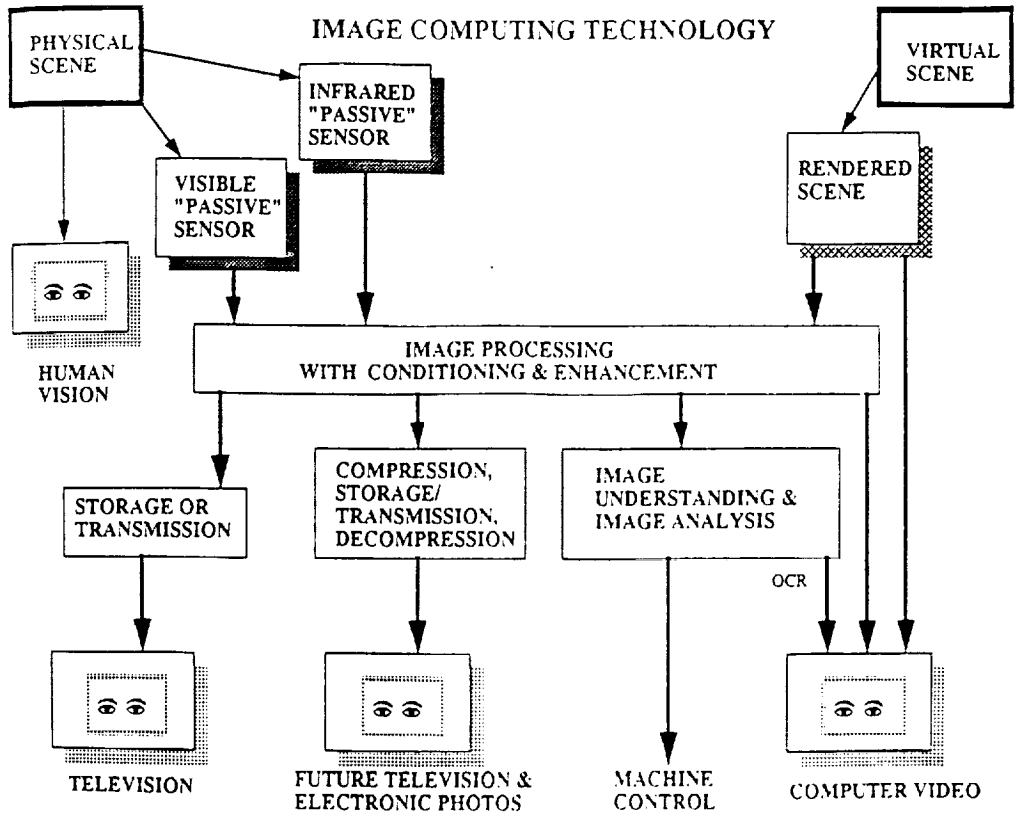

Figure 34. Image Computing Chips (after Gove)

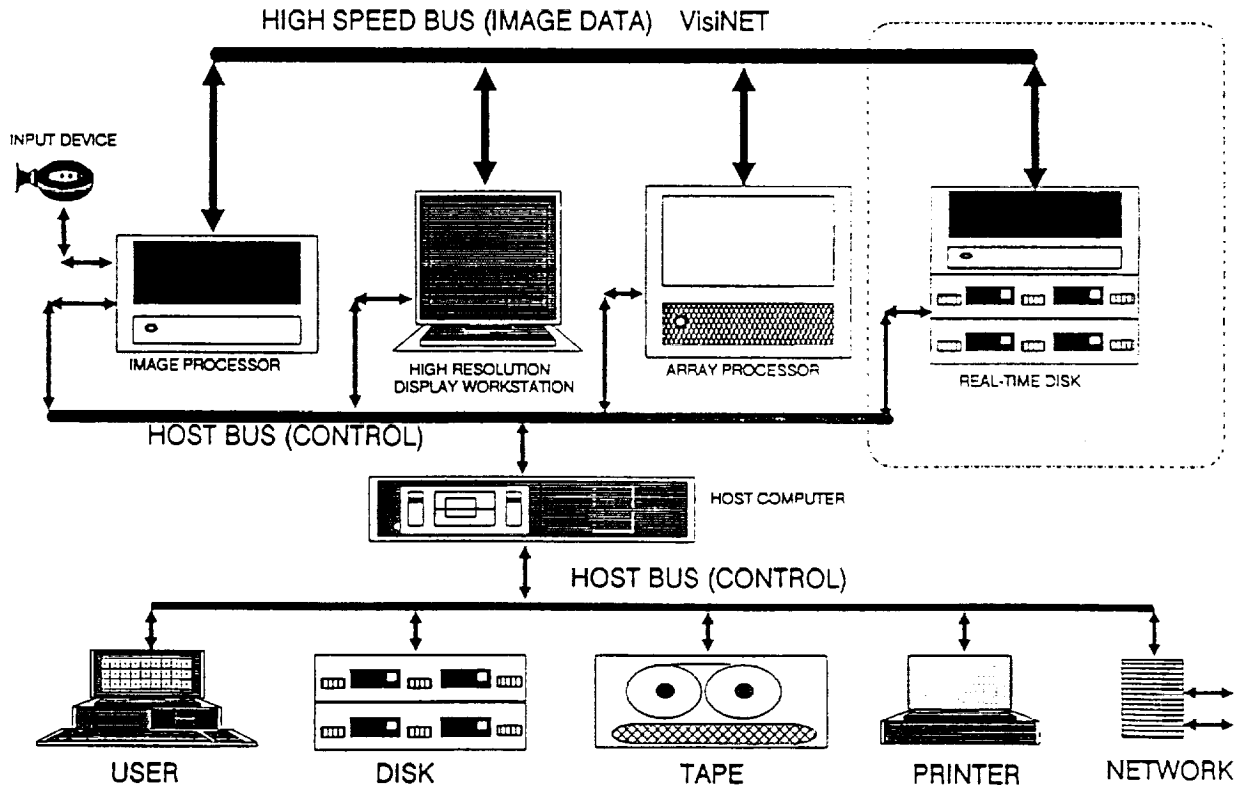

Figure 35. High Speed Networking (after Mulgronkar)

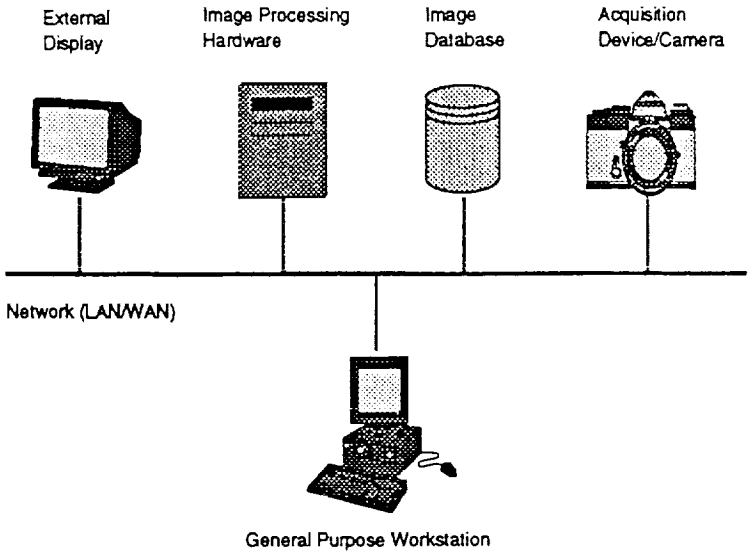

An open, distributed environment for imaging

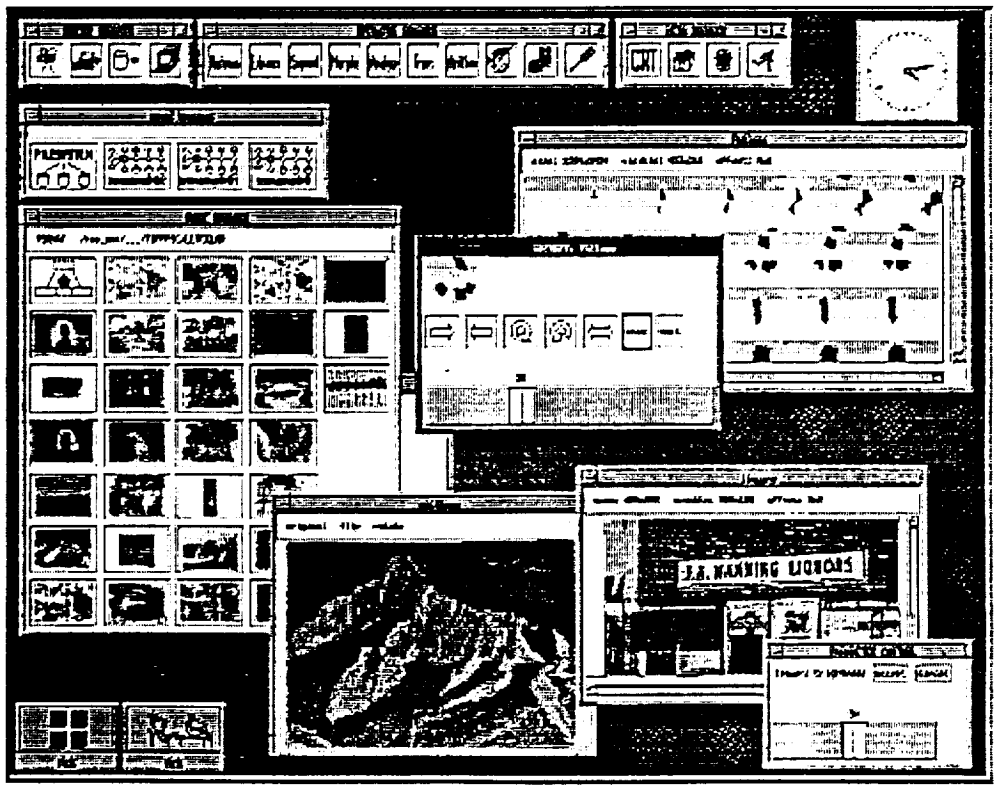

Layout of the user interface

Figure 36. "apART" Network (after Schneider)

IMAGING SUBSYSTEMS

RESOLUTION	FEATURES	COSTS
512 X 512 X 8	Capture, pseudo-color, zoom CPU for processing, 1 - 2 pages image memory	$1.2K - $2K
512 X 512 X 8	As above plus array processing, 2-4 pages image memory, non real-time convolution, real-time histogram	$4.5K -$ 9K
512 X 512 X 8	Real-time convolution, image arithmetic	$9K - $15K
512 X 512 X 16	NTSC/RGB color capture and display, no look-up tables	$1.5K - $3K
512 X 512 X 24(32)	RGB planed, look-up tables	$5K - $7K
1,024 X 1,024 X 8	No capture, LUTS. pan zoom	$2.5K - $3.5K
1,024 X 1,024 X 8	Capture subsystems (no camera)	$2.5K - $4K
2,048 X 1,536 X 8	Gray scale monochrome, no pan or zoom	$7K

Table I. Imaging Subsystems (after Strum)

Some Multifunction Digital Image and/or Graphics Processor Chips:

Name	Company	Architecture of Each Chip	Most -Suited Applications
CAAPP	Hughes	SIMD, fine grain, bit-serial processors, 4way bit mesh	low-level image processing
CytoComputer	ERIM	pipeline image processor, 8-bit ALU	neighborhood processing
DSP 56K, 96K	Motorola	Harvard RISC processor, FPU	filters, FFT
DVI i750-next	Intel	(internal) SIMD processors	video conferencing
GAPP	Martin/NCR	SIMD, 6x12 PEs,4way mesh-connected. 1-bit ALU	image processing
IP9506	Toshiba	SIMD, 3 stage pipe, 1 PE/chip	low-level image processing
i860	Intel	RISC (integer, FPU, and graphics units)	image and graphics
iWARP	Intel	fine grain parallel processor,	image processing
PIPE	ASPEX	pipelined, LUT processor	low-level image processing
SVP	TI	SIMD bit-serial video-row processors	low-level video
TMS 34020/82	TI	CISC graphics, with BitBlt and FPU	2D and 3D graphics
TMS 320C40	TI	DSP, 6way mesh-connected, 1 proc/chip (MIMD in system)	image or graphics processing
T800 Transputer	Inmos	4way mesh-connected, 1 proc/chip, FPU (MIMD in system)	image or graphics processing
Vision Processor	IIT	RISC with multiple execution units, 2 chip	video compression

Table II. Current Processor Chips (after Gove)